Splitting of ν_2 vibrational mode of CO_2 isotopic species in the unstable trapping site in argon matrix

P.R. Dahoo[a], I. Berrodier, V. Raducu, J.L. Teffo, H. Chabbi, A. Lakhlifi[b], and L. Abouaf-Marguin

Laboratoire de Physique Moléculaire et Applications[c], Université P. et M. Curie, Tour 13, Boîte 76, 4 place Jussieu, 75252 Paris Cedex 05, France

Abstract. FTIR spectra of the antisymmetric stretch ν_3 and symmetric bending ν_2 vibrational modes of isotopic species of CO_2 trapped in argon matrix are recorded at 5 K with a resolution of 0.15 cm^{-1}. A splitting of the ν_2 mode is observed for the different species in the trapping site termed unstable. Considering this splitting and the width of the ν_3 line observed for this unstable site, one expects this site to be larger than the stable one. A theoretical model is elaborated to interpret this splitting. Calculations performed at harmonic level of approximation for vibrational modes in a single substitutional site (S1) and a double substitutional one (S2) in a fcc distorted argon lattice to minimize the free energy of the molecule-matrix system, show the splitting to occur in the larger site. The latter result leads us to invert former attribution of the sites: the stable site is a single substitutional one, whereas the unstable site is a double substitutional one.

PACS. 33.20.Tp Vibrational analysis – 33.70.Jg Line and band widths, shapes, and shifts – 78.30.-j Infrared and Raman spectra

1 Introduction

Collision-induced vibrational energy transfer of $^{13}C^{16}O_2$ in argon solid matrix has recently [1,2] been investigated by laser induced fluorescence (LIF). Experiments were performed on the heavier isotopic species to avoid difficulties related to atmospheric absorption. After excitation of the ν_3 vibrational mode of the molecule, a strong emission in the 16 μm spectral region is observed. This emission exhibits a sharp threshold as a function of the laser excitation and is interpreted as the signature of vibrational stimulated emission (VSE). The emission spectrum consists of 3 lines which are assigned to $11^10(2) \rightarrow 02^20(1)$, $11^10(2) \rightarrow 10^00(2)$ and $10^00(2) \rightarrow 01^10(1)$ vibrational transitions of $^{13}C^{16}O_2$. Site selective excitation (S1 and S2 to be described below) reveals marked differences in threshold, temporal behavior and relative intensities of VSE.

The time and temperature dependence of VSE gives some insight on the vibrational dynamics of matrix iso-lated CO_2. To interpret correctly the coupling scheme leading to the observed LIF results, the nature of sites S1 and S2 must be correctly determined. In this respect, this work is devoted to the study of the sites, through observed and calculated vibrational IR spectra of CO_2.

Carbon dioxide is a linear triatomic molecule which has been studied by infrared and Raman spectroscopy [3–7] when isolated in inert matrices. For $^{12}C^{16}O_2$ in argon, the antisymmetric vibrational stretching mode ν_3 is observed as a doublet [3], a high frequency component (HF at 2345.1 cm^{-1}) separated by 6.1 cm^{-1} from the low frequency (LF at 2339.0 cm^{-1}) one. The ν_2 symmetric bending mode also appears as a doublet, the LF line (663.4 cm^{-1}) being 1.6 cm^{-1} apart from the HF line (665.0 cm^{-1}) [3]. Guasti *et al.* [5] were the first to show that these doublets are due to molecules trapped in two sites of different stabilities. For each mode, one line disappears after the matrix is strongly annealed above 35 K, the HF line for ν_2 and the LF line for ν_3. This result shows a correlation between the latter lines and the corresponding trapping site was termed unstable in opposition to stable for the other site. In a more detailed study, these results were later confirmed by Irvine *et al.* [6], for $^{13}C^{16}O_2$, $^{12}C^{16}O^{18}O$ and $^{13}C^{16}O^{18}O$. Moreover, by considering the distances between the oxygen atoms of CO_2, and the argon atoms of the matrix, in a single (S1) and a double (S2) substitutional sites, they suggested, using qualitative arguments, that S2 corresponds to the stable

[a] *Present address*: Laboratoire de Magnétisme et d'Optique de Versailles, Bâtiment Fermat, 45 avenue des États-Unis, 78035 Versailles, France.
e-mail: `prd@physique.uvsq.fr`
[b] *Present address*: Laboratoire de Physique Moléculaire, UMR CNRS 6624, UFR Sciences et Techniques, La Bouloie, Université de Franche-Comté, 25030 Besançon Cedex, France.
[c] UPR CNRS 136

site and S1 to the unstable one. In S1, the molecular axis is along the fourfold axis (the 100 or equivalent plane) of the matrix and in S2, the center of mass of the molecule is at the center of a nearest-neighbor double substitutional site. In a recent publication, Nxumalo and Ford [7] who studied CO_2 and N_2O dimers in argon and nitrogen matrices at 17 K, reported three frequencies from weak asymmetric structures at the foot of a saturated line. The structures showing no intensity change after strong annealing, they were attributed to site effects on the ν_2 mode of the monomer $^{12}C^{16}O_2$ without any other comments.

The experimental part of this work (Sect. 2) concerns line positions of ν_2 and ν_3 modes of isotopic species, prepared from ^{12}C, ^{13}C, ^{16}O, ^{17}O and ^{18}O atoms, trapped in argon matrix in sites S1 and S2. The aim is to study, at high resolution, site effects on the degenerate ν_2 vibrational mode of CO_2. After a brief description of the experimental method, we present results obtained at a resolution of 0.15 cm^{-1} at 5 K, followed by a discussion on the possible trapping sites and their nature.

In Section 3, a theoretical model elaborated to calculate the frequencies of low lying vibrational levels of a linear triatomic molecule embedded in a matrix is described and results of calculations carried at the harmonic approximation level are given. In particular, we show that the attribution of sites S1 and S2 of reference [6] ought to be inverted.

2 Experimental

2.1 Set up and procedure

The experimental setup and cryogenic system has already been described in reference [8]. The CO_2:argon gas mixture, at the required dilution (RG/M=Ar/CO_2=1000, in the present work) is prepared by standard manometric techniques. It is then sprayed, at the rate of a few millimoles per hour, on a gold-plated copper mirror kept at the optimized deposition temperature of 20 K for argon matrix. Infrared spectrum of the sample is recorded by means of a FTIR spectrometer from Bruker (IFS 113V). Spectra of 0.15 cm^{-1} resolution are collected at regular intervals to check that absorption of CO_2 remains linear during the crystalline matrix growth. A DTGS detector is used to collect data and software from Bruker allows for spectrum analysis.

After deposition, the sample holder, fixed at the bottom of a circulating liquid helium cryostat, is gradually cooled to 5 K. The sample is then annealed at a temperature lower than 35 K, before being cooled back to 5 K. A carbon sensor embedded within the mirror body allows temperature measurements between 5 K and 20 K, while temperatures above 20 K are measured by means of a platinum resistance thermometer. For each dilution, the deposited sample thickness is chosen so that the best experimental conditions are achieved, that is good signal to noise ratio and absorptions far from saturation (optical density lower than 0.4) to stay in the linear response of the spectrometer and get reliable measurements of the
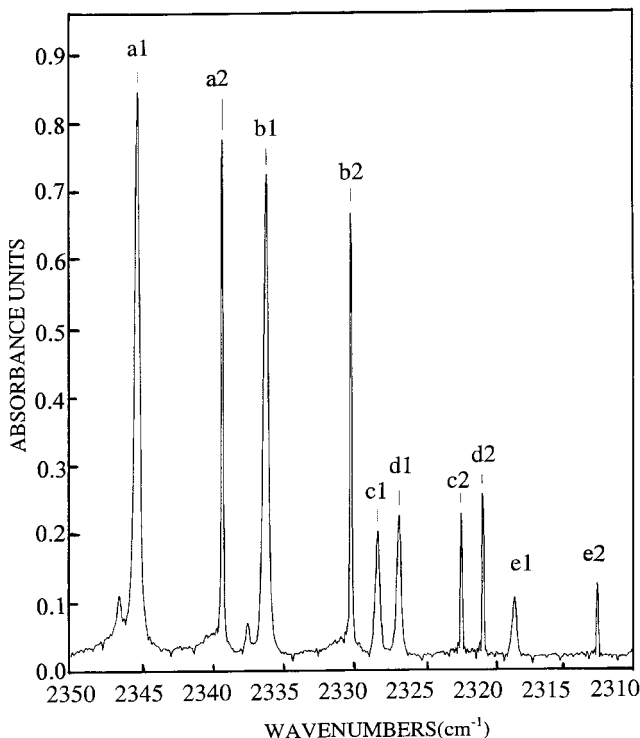

Fig. 1. Infrared absorption spectrum of CO_2 in solid argon (M/R = 1000, T = 5 K, resolution = 0.15 cm^{-1}) in the ν_3 stretching region (1 = stable site; 2 = unstable site; a = 626, b = 627, c = 628, d = 727, e = 728).

line intensities and full widths at half maximum (FWHM). Typically 100 scans are necessary.

2.2 Results and discussion

In Figures 1 and 2 are shown the spectra observed at 5 K, in the ν_3 and ν_2 vibrational modes absorption domain respectively, for five different isotopes. The sample dilution RG/M is 1000 and the sample's thickness is 95 μm (70 torr deposited). This thickness is determined from a calibration obtained once for the argon matrix by counting interference fringes of a He–Ne laser, recorded during deposition. In Figure 1 one finds a series of doublets for the ν_3 mode corresponding to the absorption of the different isotopic species, the HF line having a FWHM (0.39 cm^{-1}) is broader than the LF line (0.15 cm^{-1}, the experimental resolution). In the case of $^{13}C^{16}O_2$, this width has been measured to be 0.13 cm^{-1} (0.03 cm^{-1} resolution) [9]. For ν_3 lines of optical density higher than 0.4, only 26 torr of the sample was deposited. In Figure 2, instead of a series of doublets, three lines can be attributed to the ν_2 mode of the monomer CO_2 for each isotopic species. At the resolution of 0.15 cm^{-1}, a splitting of the HF line is observed for the five species.

Considering the results of Guasti *et al.* [5] and Irvine *et al.* [6] about the unstable site, we checked on $^{13}C^{16}O_2$ isotopic species that the unstable site disappears after
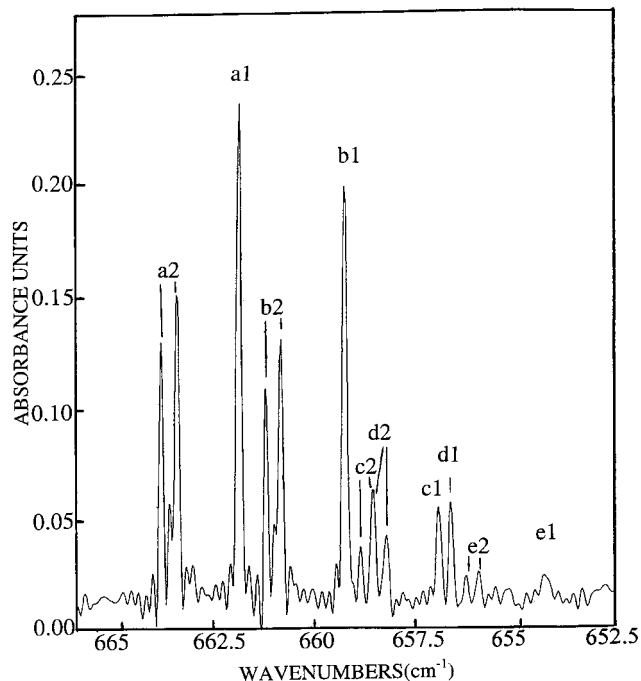
Fig. 2. Infrared absorption spectrum of CO_2 in solid argon (M/R = 1000, $T = 5$ K, resolution = 0.15 cm^{-1}) in the ν_2 bending region (1 = stable site; 2 = unstable site; $a = 626$, $b = 627$, $c = 628$, $d = 727$, $e = 728$).

strong annealing. In contrast, if annealing is mild, no measurable effect on the line intensities and widths are observed for molecules absorbing in both sites. Moreover, for temperatures ranging from 5 K to 25 K, the line width of the ν_3 mode remains unchanged for molecules absorbing in the unstable site (0.13 cm^{-1}) and varies only slightly for those in the other site (0.35 cm^{-1} to 0.38 cm^{-1}). So if the temperature of the matrix is kept below 25 K the two observed sites can be considered as being both stable. One may note that when the deposition temperature is decreased from 20 K (the optimum temperature for the argon matrix) to 10 K, the intensity and the width of the line corresponding to the unstable site increase. The width decreases after mild matrix annealing showing that other possible unstable sites can trap $^{13}C^{16}O_2$ under such experimental conditions [9].

Spectra recorded for different RG/M ratio (200, 500, 1000, 2000, 3500, 5000) show dimers to be present in the matrix for ratio smaller than one thousand. The lines corresponding to the absorption of the dimers appear on the side of those pertaining to the monomers. For the latter, the splitting of the ν_2 mode in the unstable site is still observed whatever the RG/M ratio. No other trapping site is observed.

The frequencies observed at 5 K for the ν_2 bending and the ν_3 antisymmetric vibrational modes are given in Table 1. For simplification, instead of the full isotopic notation, we use the short cut convention, 626 for $^{12}C^{16}O_2$, 636 for $^{13}C^{16}O_2$, 627 for $^{16}O^{12}C^{17}O$ and so on. The re-

sults are compared to the most recent available ones for isotopic species already studied [6].

To our knowledge, no splitting of the HF component of the ν_2 mode (unstable site), has been reported before. It was probably not observed because of the lower resolution (1 cm^{-1} to 0.5 cm^{-1}) at which the spectra [3–7] were recorded. Considering this splitting, it is reasonable to assume that the interaction between the molecule and the matrix atoms must be more anisotropic in the unstable site than in the stable one. Furthermore, the fact that this line is correlated to the LF component of the ν_3 mode, which has a FWHM narrower than that of the corresponding HF line (stable site), leads one to consider an unstable site which is larger in size than the stable one. Indeed, in a large site, the coupling of the vibrational degrees of freedom with the matrix atoms must be weaker than in a small site, namely if one considers the repulsive part of the interaction. This could explain why the line widths of the ν_3 mode are different by a factor of 3 in the two trapping sites.

To determine the nature of these sites, we may refer to the suggestion of Irvine *et al.* [6]. In S1 (single site) of O_h symmetry, the molecule is along one of the fourfold axes in a face-centered-cubic (fcc) lattice. In S2 (double site), the molecule is at the center of a nearest-neighbor double substitutional site which is now of D_{2h} symmetry. If we look at the degenerate bending ν_2 mode as two vibrations occurring in two perpendicular planes containing the molecular axis, then, in the perfect crystal, the matrix effect should be the same for both vibrations in S1, owing to its O_h symmetry. In contrast, because of the symmetry of site S2, the matrix environment is not equivalent for the two perpendicular ν_2 mode vibrations and one therefore expects the degeneracy of the ν_2 mode to be lifted. Although the lattice distorts locally to minimize the total energy of the crystal as CO_2 replaces one or two argon atoms, the matrix environment effect should not be too different from that of the otherwise perfect crystal. So the attribution of Irvine *et al.* [6] ought to be inverted: the stable site in which no splitting is observed is S1, the single substitutional one, whereas the unstable site, in which ν_2 mode splits and ν_3 line is narrower, is S2, the double substitutional one.

3 Theoretical model

To test the validity of this proposed attribution and to calculate the vibrational energy of low lying levels of the trapped molecule, we have elaborated a theoretical model so as to allow an overall treatment of vibrational degrees of freedom as it is done in gas phase [10,11].

This model (M2) is an extension of the site inclusion model (M1) used to study O_3 [12] and C_3 [13] trapped in rare gas matrices and which is built on the Born-Oppenheimer approximation, allowing a decoupling of the vibrational degrees of freedom (high frequency motions) from orientational and translational degrees of freedom (low frequency motions) of the molecule-matrix system.

Table 1. Fundamental vibrational frequencies (in cm^{-1}) of isotopic species of CO_2 monomers in argon matrix (resolution = 0.15 cm^{-1}, $T = 5$ K, RG/M = 1000).

Isotopic species[a]	Site S1 stable S2 unstable	This work resolution = 0.15 cm^{-1} $T = 5$ K		Reference [4] resolution = 0.5 cm^{-1} $T < 10$ K	
		ν_2	ν_3	ν_2	ν_3
626	S1	661.9	2345.1	661.8	2345.2
	S2	663.4	2339.0	663.3	2339.1
	S2	663.8	–	–	–
627	S1	659.2	2335.9	–	–
	S2	660.8	2330.0	–	–
	S2	661.2	–	–	–
628	S1	656.8	2328.0	657.1	2329.2
	S2	658.9	2322.1	658.7	2323.3
	S2	658.5	–	–	–
727	S1	656.6	2326.5	–	–
	S2	658.5	2320.6	–	–
	S2	658.2	–	–	–
728	S1	654.2	2318.4	–	–
	S2	655.9	2312.5	–	–
	S2	656.5	–	–	–
828	S1	–	2310.0	–	–
	S2	–	2304.2	–	–
		–	–	–	–
636	S1	643.1	2279.6	643.2	2280.0
	S2	644.5	2273.7	644.6	2273.9
	S2	645.0	–	–	–
637	S1	–	2270.2	–	–
	S2	–	2264.3	–	–
		–	–	–	–
638	S1	–	–	–	2256.4
	S2	–	–	–	2262.3
		–	–	–	–

[a] Short cut notation: 626 = $^{12}C^{16}O_2$; 627 = $^{16}O^{12}C^{17}O$; 636 = $^{13}C^{16}O_2$...

It has, however, the drawback that each vibrational level has to be separately handled.

Moreover, in model M2, one can consider the orientational and translational degrees of freedom of the molecule-matrix system as a bath interacting with the vibrations of the trapped molecule. Non-radiative relaxation rate constants for any vibrational level can be calculated when the coupling of high frequency motions and low frequency ones are taken into account.

The general formalism of the model is outlined in Section 3.1, a comparison between M1 and M2 being made when they differ. The main steps involved in the calculation are described in Sections 3.1 and 3.2 and for a linear triatomic molecule such as CO_2, the method elaborated to handle the lifting of the degeneracy of the ν_2 mode is separately discussed in Section 3.3. Results are given in Section 3.4.

3.1 Site inclusion model and interaction potential energy

At cryogenic temperatures the argon matrix is a face-centered-cubic (fcc) lattice with a primitive cell parameter a equal to 3.75 Å (Tab. 2) the distance between two nearest neighbor atoms. The inclusion of the linear molecule in the matrix consists in the substitution of one atom (S1) or two adjacent (S2) (or more SN) atoms of this matrix. In practice, experiments are performed with highly diluted samples with RG/M ratio greater than 1000. So, in our calculations we assume that the trapped molecules are isolated from each other (*i.e.* no interactions exist between

Table 2. Atoms: cell parameter (a (Å)) in argon matrix, polarizabilities (α (Å^3)) and pure Lennard-Jones potential parameters (ϵ (cm^{-1}), σ (Å)) of argon, carbon and oxygen atoms. Molecules: molecular internal characteristics of the rigid molecule with respect to its frame. Bond length (q_M^e), bond angle (β_M^e), dipole μ_M^e and quadrupole $\mathbf{Q}_{zz}$ moments.

Atoms			
	C	O	Ar
a (Å)			3.75
α (Å^3)			1.64
ϵ (cm^{-1})	29.8	39.9	84.4
σ (Å)	3.21	2.88	3.45
Molecules			
	$^{12}C^{16}O_2$	$^{13}C^{16}O_2$	
q_M^e (Å)	1.16	1.16	
β_M^e (deg)	180	180	
μ_M^e (D)	0	0	
$\mathbf{Q}_{zz}$ (D Å)	-4.3	-4.3	

Fig. 3. Instantaneous geometrical characteristics of the vibrating (ν_2 mode) CO_2 in the argon matrix. $(\mathbf{X}, \mathbf{Y}, \mathbf{Z})$ and $(\mathbf{x}, \mathbf{y}, \mathbf{z})$ are the absolute and molecular frames; $(\theta, \varphi, \chi = 0)$ are the Euler angles. ξ_l ($l = 0$ or j) are the vectors defining the displacements of the center of mass or that of the argon atom j. r_{ij} is the distance between the atom i of CO_2 and the argon atom j.

guests) and therefore, we will consider the trapping of only one molecule in the matrix.

The total potential energy of such a trapped molecule-matrix system is written as:

$$V = \sum_j V_{Mj}(\mathbf{r}_{0j}) + \sum_{jj', j<j'} V_{jj'}(\mathbf{r}_{jj'}) \tag{1}$$

where the term V_{Mj} characterizes the molecule-matrix interaction which is given in equation (3) below, with $\mathbf{r}_{0j}$ being the distance vector between the molecular center of mass (c.m.) and the jth matrix atom. The second term represents the matrix-matrix interaction where $V_{jj'}$ is the potential energy between the jth and j'th RG atoms located at the $\mathbf{r}_j$ and $\mathbf{r}_{j'}$ positions with respect to the absolute frame tied to the crystal as shown in Figure 3. This last part consists of 12-6 Lennard-Jones (LJ) atom-atom contributions, only, and is given by:

$$V_{jj'}(\mathbf{r}_{jj'}) = 4\epsilon_{rg} \left(\frac{\sigma_{rg}}{\mathbf{r}_{jj'}}\right)^6 \left\{ \left(\frac{\sigma_{rg}}{\mathbf{r}_{jj'}}\right)^6 - 1 \right\} \tag{2}$$

where ϵ_{rg} and σ_{rg} are the LJ parameters of argon [14], given in Table 2.

The interaction potential energy between the trapped triatomic linear molecule and a RG atom can be written as the sum of 12-6 LJ atom-atom potentials characterizing the repulsion-dispersion contributions and an induction part due to the interaction between the permanent electric multipoles of the molecule and the dipole induced at the position of the RG atom. It can be written as:

$$V_{Mj}(\mathbf{r}_{0j}) = \sum_{i=1}^{3} 4\epsilon_{ij} \left\{ \left(\frac{\sigma_{ij}}{\mathbf{r}_{ij}}\right)^{12} - \left(\frac{\sigma_{ij}}{\mathbf{r}_{ij}}\right)^6 \right\} - \frac{1}{2}\alpha_j \mathbf{E}_{Mj}^2 \tag{3}$$

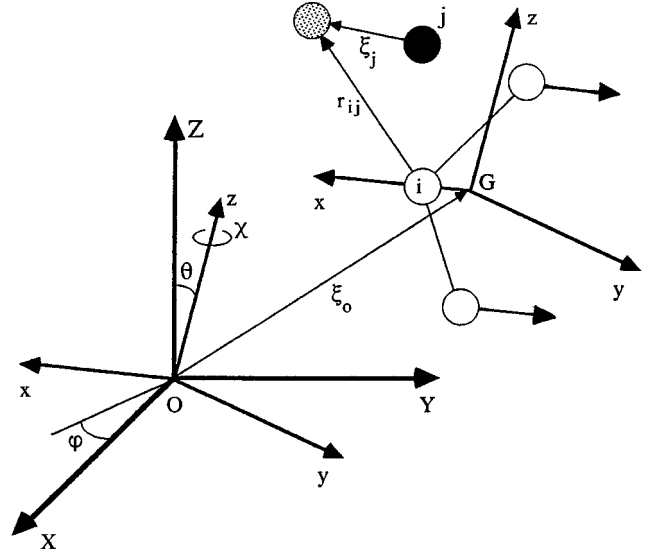where i and j characterize the ith atom of the molecule and the jth RG atom, respectively; ϵ_{ij} and σ_{ij} are the mixed LJ potential parameters obtained by using the usual Lorentz-Berthelot combination rules $\epsilon_{ij} = \sqrt{\epsilon_{ii}\epsilon_{jj}}$ and $2\sigma_{ij} = \sigma_{ii} + \sigma_{jj}$ and $\mathbf{E}_{Mj}$ is the field generated by the molecular permanent electric multipoles (μ_M, Θ_M, ...) on the rare gas atom with isotropic polarizability α_j. The distance vector $\mathbf{r}_{ij}$ between the ith atom of the molecule and the jth RG atom, can be expressed in terms of the distance vector $\mathbf{r}_{0j}$ between the molecular c.m. and the RG atom and the position vector $\mathbf{r}_i$ of the ith atom with respect to the molecular frame ($\mathbf{x}$, $\mathbf{y}$, $\mathbf{z}$). The orientational degrees of freedom Ω of the molecule ($\Omega = (\theta, \varphi)$) and the position vector of any RG atom j, are defined in the absolutecrystal frame ($\mathbf{X}$, $\mathbf{Y}$, $\mathbf{Z}$) as shown in Figure 3. The rotational matrix transformation following Rose convention [15], is used to change from the crystal absolute frame to the molecular frame. The LJ potential parameters and isotropic polarizabilities for the carbon [16], oxygen [17] atoms in CO_2 and for the rare gas atoms are given in Table 2 together with the internal characteristics for the rigid linear molecule [18,19].

The incorporation of the guest molecule in a substitutional site of the fcc host crystal is generally responsible for more or less important anisotropic distortions of the atoms around their perfect crystal positions. These distortions strongly depend on the size and shape of the molecule and the site (single, double, ...), on the one hand, and on the rigidity of the matrix and the experimental preparation conditions of the sample, on the other hand. They are expressed in terms of displacement vectors of the molecular c.m. and of the matrix atoms corresponding to

the distortion of the molecule-matrix system. The latter vectors are calculated on the basis of the Green tensor of the perfect crystal by solving a system of equations which satisfy the minimum energy condition for the doped crystal, following the method of Flinn and Maradudin [20] developed to study impurities trapped in solids. With ξ_l denoting the instantaneous displacement vector connected to the lth particle ($l = 0$ for the molecular c.m. and j for the matrix atoms), it can be expressed as

$$\xi_l = \xi_l^s(\Omega, \{Q\}) + u_l \tag{4}$$

where ξ_l^s characterize the static displacement vectors which depend on the molecular orientation Ω and internal vibration $\{Q\}$ motions. However, as this dependence remains weak when the molecule moves about its equilibrium orientation Ω^e and internal vibrations $\{Q^e\}$, one can replace $\xi_l^s(\Omega, \{Q\})$ by $\xi_l^s(\Omega^e, \{Q^e\})$ to determine the interaction potential energy between the molecule and the matrix. In equation (4) the **u** vectors define the dynamical external motions of the lattice atoms and the molecular c.m. They can be ignored for the calculations of the energy levels and transition moments.

Considering the results obtained for O_3 [12] and C_3 [13], we have tried various trapping sites and as for these molecules the most probable sites corresponding to a minimum in the evaluation of the energy of the molecule-matrix system, are: (i) the single substitutional site (S1) in which only the central RG atom of the crystal is replaced by the molecule (see Fig. 4a) and (ii) the double substitutional site (S2) where the central atom and one of the nearest neighbor atoms are replaced by the molecule. For this case the site center is located between these two atoms (see Fig. 4b). One may note that these sites correspond to those proposed by Irvine *et al.* [6]. Results concerning these calculations are given below in Section 3.4.

In the rigid distorted crystal approximation, the potential energy hypersurface experienced by the molecule in its site n can then be written as:

$$V_M^{(n)}(\xi^s, \Omega, \{Q\}) = V_M^{(n)e}(\xi^s) + V_M^{(n)}(\xi^s, \{Q\})$$
$$+ V_M^{(n)}(\xi^s, \Omega) + \Delta V_M^{(n)}(\xi^s, \Omega, \{Q\}) \tag{5}$$

where:

- $V_M^{(n)e}(\xi^s)$ is the minimum of the potential energy corresponding to the equilibrium configuration;
- $V_M^{(n)}((\xi^s), \{Q\})$, is the vibrational dependence in terms of normal coordinates $\{Q\}$;
- $V_M^{(n)}((\xi^s), \Omega)$, is the orientational dependence in terms of Euler angles ($\Omega = (\theta, \varphi, \chi)$, $\chi = 0$ for a linear molecule);
- $\Delta V_M^{(n)}((\xi^s), \Omega, \{Q\})$, is the vibration-orientation coupling term, which induce the relaxation of vibrational modes onto orientational modes;
- and n characterizes the trapping site ($n = 1$ for S1 and $n = 2$ for S2). The parameter ξ^s represents the
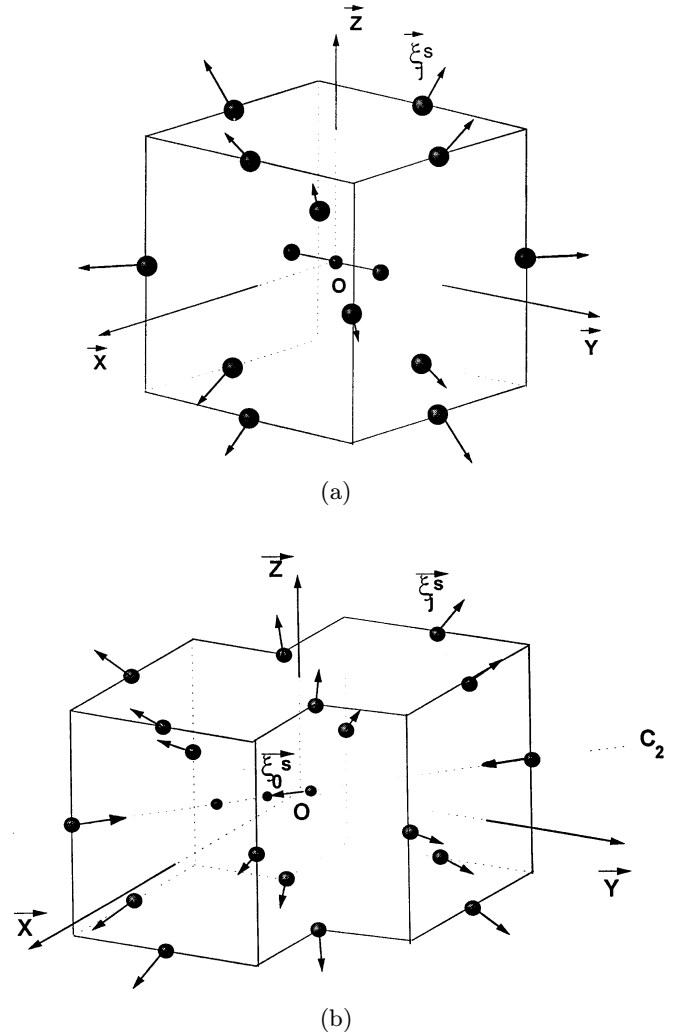

(a)

(b)

Fig. 4. Equilibrium characteristics of isolated CO_2 in solid argon. Molecular orientation and static displacements of the molecular center of mass and the first shell matrix atoms in S1, the single (a) and S2, the double (b) substitutional sites.

displacement vectors of the RG matrix atoms and the center of mass of the trapped molecule, determined by the Green functions of the perfect crystal (Eqs. (4, 5) of Ref. [12]).

3.2 Molecular Hamiltonian of the trapped molecule

The rovibrational Hamiltonian H of the isolated molecule in gas phase is generally expanded in terms of dimensionless vibrational normal coordinates, their conjugate momenta and rotational momenta and is written as shown below:

$$H = H_0 + H_1 + H_2 + ... \tag{6}$$

with H_0, H_1 and H_2 given by (only vibrational terms are given for orders higher than zero):

$$H_0 = \frac{1}{2}\sum_i w_i(p_i^2 + q_i^2) + \sum_\alpha B_\alpha J_\alpha^2 \qquad (7)$$

$$H_1 = \sum_{ijk} k_{ijk}q_iq_jq_k + ... \qquad (8)$$

$$H_2 = \sum_{ijkl} k_{ijkl}q_iq_jq_kq_l + ... \qquad (9)$$

In the above expressions, the first term in H_0 is the harmonic contribution of the vibrational energy (the harmonic oscillator operator) and the remaining term is the rigid rotor operator. q_i and p_i are the ith vibrational normal coordinate and its conjugate momentum operator and J_α is the angular momentum operator. ω_i is the frequency corresponding to the ith oscillator and B_α is the rotational constant corresponding to J_α, both expressed in cm^{-1}. H_1 and H_2 describe the anharmonicities of vibrations with the corresponding force constants k_{ijk} and k_{ijkl}. These constants correspond to dimensionless normal coordinates q_i which are related to normal coordinates Q_i by the following expression:

$$q_i = \frac{\lambda_i^{1/4}}{\hbar^{1/2}}Q_i \qquad (10)$$

where $\sqrt{\lambda_i} = 2\pi c\omega_i$ is the frequency of the normal vibration described by Q_i. The normal coordinates allow simultaneous diagonalization of the kinetic energy operator and the potential energy operator in the harmonic approximation. They are related to $\sqrt{m_k}\delta\alpha_k$, the mass weighted Cartesian displacement of the kth atom of the vibrating molecule by the following equation:

$$\sqrt{m_k}\delta\alpha_k = \sum_i l_{ki}^\alpha Q_i \qquad (11)$$

which can be written in matrix form as

$$\delta\alpha = M^{-1/2}lQ \qquad (12)$$

where M is a $3N \times 3N$ diagonal matrix, l is the matrix used by Nielsen *et al.* [11] and $\delta\alpha$ and Q are vectors with $3N$ and $3N-6$ elements respectively. Note that this matrix can be determined by standard Wilson's GF method [20].

The rovibrational Hamiltonian of the molecule inside the matrix in site S1 or S2, is thus written as the sum of the Hamiltonian of the isolated molecule in gas phase (Eqs. (6–9)) and the potential in equation (5). $V_M^{(n)e}(\xi^s)$ being a constant term, it can be omitted from the Hamiltonian expression as only energy difference of the vibrational levels are evaluated. $V_M^{(n)}((\xi^s), \{Q\})$ is the vibrational part of the interaction potential which can be expanded as a Taylor series in terms of dimensionless vibrational normal coordinates $\{q\}$. $V_M^{(n)}((\xi^s), \Omega)$ is the orientational part which can also be expanded in terms of adapted Euler angles dependent variables. The vibration-orientation term $\Delta V_M^{(n)}(\xi^s, \Omega, \{Q\})$, is neglected in the

Born-Oppenheimer approximation. Since we are only interested in the study of the vibrational degrees of freedom of the trapped molecule, only the vibrational part of this Hamiltonian will be considered in what follows.

As experiments shows vibrational shifts to be small, $V_M^{(n)}((\xi^s), \{Q\})$ is expanded up to second order only as:

$$V_M^{(n)}(\xi^s, \{Q\}) = \sum_i \beta_i q_i + \sum_i \sum_{j>i} \beta_{ij} q_i q_j \qquad (13)$$

where q_i are dimensionless normal coordinates given by equation (10) and β_i and β_{ij} are first and second derivatives of V_M with respect to coordinates q_i. Then the nuclei, because of the matrix effect, are moving in a mean force field, gradient of a perturbed potential given by:

$$U(\{q\}) = \sum_i \frac{\omega_i}{2}q_i^2 + H_1 + H_2 + \sum_i \beta_i q_i + \sum_i \sum_{i<j} \beta_{ij} q_{ij} \qquad (14)$$

and whose minimum corresponds to a new stable equilibrium configuration of the nuclei.

In model M1, vibration-translation coupling is taken into account and each vibrational state is separately handled. The mean distances between the atoms in the molecule are calculated and the equilibrium configuration determined for each vibrational state. The various terms in equation (13), which are different for each state, are then incorporated in standard Rayleigh-Schrödinger perturbation theory to determine the mean energy of the molecule in each state. The energy differences between the calculated vibrational energy levels are then compared to the corresponding observed transitions. For the three rare gas matrices (argon, krypton and xenon), the relative shifts are comparable for ν_3 vibrational mode of O_3 [12], but this method is not convenient for calculating the energies of low lying vibrational levels although site effects such as the splitting of degenerate vibrational modes can be determined by this model as it was shown for ν_2 vibrational mode of linear C_3 in RG [13].

In the present model M2, we develop a different method also based on the Born-Oppenheimer approximation which allows low frequency motions (orientational and translational) to be separated from high frequency ones (vibration). But the molecule is instead considered to be moving in a cell under the influence of the electric field due to the surrounding distorted polarized matrix atoms. A global treatment of the vibrational degrees of freedom can thus be undertaken. Defining the origin of $U(\{q\})$ at this minimum, and after applying an orthogonal transformation to the transformed Hamiltonian to eliminate cross terms $\beta'_{ij}(i \neq j)$, the Hamiltonian of the trapped molecule in its ground electronic state and in the new equilibrium position of the vibrating nuclei is written as:

$$H'_0 = \frac{1}{2}\sum_i \omega'_i(p'^2_i + q'^2_i) \qquad (15)$$

$$H'_a = \sum_{ijk} k'_{ijk}q'_iq'_jq'_k + \sum_{ijkl} k'_{ijkl}q'_iq'_jq'_kq'_l + ... \qquad (16)$$

Perturbation theory can then be applied to H'_a using contact transformation method [10,11].

The harmonic oscillator wavefunctions of H'_0 are used as basis functions to calculate the energies in the zeroth order. Higher orders are treated by application of successive unitary transformations $U_n = \exp(iS_n)$, where S_n is a hermitian operator, to H' [22,23].

Up to second order, for an arbitrary number of non-degenerate oscillators, the vibrational energy is written as:

$$G(v) = \sum_i \omega'_i \left(v_i + \frac{1}{2}\right) + \sum_{i \leq j} x_{ij} \left(v_i + \frac{1}{2}\right)\left(v_j + \frac{1}{2}\right) \quad (17)$$

where ω_i are the zeroth order vibrational frequencies and x_{ij} are the anharmonic constants expressed in terms of cubic and quartic potential constants.

However as for model M1, only relative shifts and degeneracy lifting are correctly reproduced for the different rare gas matrices (Ar, Kr and Xe). This can be understood if one admits that the matrix distortion as determined by the Green functions of the perfect crystal is only approximate since it corresponds to the minimization of the internal energy of the molecule-matrix system instead of that of the free energy. So, to at least determine the mean distortion around any one molecule trapped inside the solid matrix, we use an iterative procedure using alternatively FORTRAN and MAPLE code programs to adjust the observed shift of the antisymmetric vibrational fundamental mode (the strongest line in the absorption spectrum) and the calculated one at the harmonic level. This iteration starts with the initial matrix distortion as calculated by the Green functions of the ideal matrix and is stopped when the fit is achieved.

3.3 Vibrational frequencies of the ν_2 degenerate mode

The eigenvalue equation for the vibrational Hamiltonian in equations (7–9) may be solved using perturbation theory in the frame of the contact transformation method, but contrary to the gas phase triatomic case the zeroth order Hamiltonian contains four non degenerate normal vibrations (for molecules trapped in S2) yielding a four dimensional harmonic basis $|v_1, v_2, v_3, v_4\rangle$. The corresponding zeroth order energies are given by the first term in equation (17). For example the energies of the $|0, 1, 0, 0\rangle$ and $|0, 0, 1, 0\rangle$ levels are respectively:

$$E_2^0 = (1/2)(3\omega'_2 + \omega'_3) + (1/2)(\omega'_1 + \omega'_2),$$
$$E_3^0 = (1/2)(3\omega'_3 + \omega'_2) + (1/2)(\omega'_1 + \omega'_4). \quad (18)$$

It is easy to show that this result can be obtained through degenerate perturbation theory using the three dimensional Wang basis [24]

$$|v_1, v_2, |\ell|, v_4\rangle_\pm = (1/\sqrt{2})\Big[|v_1, v_2, +\ell, v_4\rangle_\pm |v_1, v_2, -\ell, v_4\rangle\Big], \quad (19)$$

which splits the Hamiltonian matrix of linear molecules into two blocks of so-called e and f parities [24].

The zeroth order Hamiltonian in equation (15) can be rewritten as (in wavenumbers units)

$$H'_0 = (1/2)\left[\omega'_1(p'^2_1 + q'^2_1) + \bar{\omega}_2(p'^2_2 + p'^2_3 + q'^2_2 + q'^2_3) + \omega'_4(p'^2_4 + p'^2_4)\right] + (1/2)\delta_2(p'^2_2 - p'^2_3 + q'^2_2 + q'^2_3) \quad (20)$$

with

$$\bar{\omega}_2 = (1/2)(\omega'_2 + \omega'_3); \quad \delta_2 = (1/2)(\omega'_2 - \omega'_3). \quad (21)$$

The first term in equation (20) is the zeroth order Hamiltonian $\bar{H}_0$ of the linear triatomic molecule having the degenerate bending mode frequency $\bar{\omega}_2$. Thus, this operator is purely diagonal in the basis of equation (19) and the corresponding zeroth order energies are:

$$\bar{E}_0(v_1, v_2, v_4) = \omega'_1(v_1 + 1/2) + \bar{\omega}_2(v_2 + 1) + \omega'_4(v_4 + 1/2). \quad (22)$$

The second term in equation (20) may be considered as a perturbation V'_0. The non-vanishing matrix elements of V'_0 in the Wang basis are:

$$\langle v_1, v_2, 0, v_4|V'_0|v_1, v_2, 2, v_4\rangle_+ = -\delta_2\sqrt{\frac{v_2(v_2 + 2)}{2}}; \quad v_2 \text{ even}; \quad (23)$$

$$\pm\langle v_1, v_2, 1, v_4|V'_0|v_1, v_2, 1, v_4\rangle_\pm = \mp\frac{\delta_2}{2}(v_2 + 1); \quad v_2 \text{ odd}; \quad (24)$$

$$\pm\langle v_1, v_2, \ell, v_4|V'_0|v_1, v_2, \ell + 2, v_4\rangle_\pm = -\frac{\delta_2}{2}\sqrt{\frac{(v_2 - \ell)(v_2 + \ell + 2)}{2}}; \quad \ell > 1. \quad (25)$$

Thus the degeneracy of the $|0, 1, 1, 0\rangle_\pm$ level is split by the perturbation V'_0, and the two corresponding energies are obtained by adding equations (22–24), which immediately gives the result found in equation (18), the $|0, 1, 1, 0\rangle_-$ and $|0, 1, 1, 0\rangle_+$ levels having the energies E_2^0 and E_3^0 respectively.

3.4 Calculations and discussion

In this section, we give results obtained at zeroth order for ν_2 and ν_3 modes. The model has been applied at the harmonic approximation level for $^{12}C^{16}O_2$ and $^{13}C^{16}O_2$ in argon. Only the equilibrium configuration of the molecules in the different trapping sites (S1 and S2) and site effects are presented in this work. Results of calculations of the vibrational energies and the transition moments from application of contact transformation method will be given in a forthcoming paper for low lying levels of the molecules trapped in argon, krypton and xenon matrices.

Table 3. Equilibrium characteristics of CO_2 molecule trapped in sites S1 and S2 in argon matrix (S1 single substitutional and S2 double substitutional sites).

Trapping Site	$n = 1$	$n = 2$
	S1	S2
φ^e	0	$-\pi/4$
θ^e	0	$\pi/2$
ξ_1^s (Å)	0.28	0.11
ξ_0^s (Å)	0.00	0.92
$V_M^{(n)e}$ (cm^{-1})	-1993	-2010

3.4.1 Equilibrium characteristics

The first step in the calculations consists in determining the most probable trapping sites of the triatomic linear molecule in the argon matrix. In the perfect face-centered-cubic (fcc) structure of the matrix, two trapping sites have been considered: the single S1 and double S2 substitutional sites described above and which correspond to those discussed by Irvine *et al.* [6].

To simulate dilute experimental conditions, 1060 RG atoms around the trapped molecule, which corresponds to 32 shells in the perfect crystals, have been taken in account. For each molecule-matrix system (S1 and S2), a set of different orientations $\Omega = (\theta, \varphi)$ of the trapped molecule is considered to determine the distortion vectors (ξ_0 and ξ_l for the molecular c.m. and every RG atoms given in equation (4) which minimize the total potential energy of the doped crystal and defined in equation (5). The calculated distortion vectors are then used to determine the potential energy surfaces experienced by the molecule in its trapping site (see Eq. (5)).

In this preliminary study we find that the minimum of the total potential energy is obtained for the S1 and S2 substitutional sites with anisotropic distortions of the argon atoms around the trapped molecule. In Table 3 we give the equilibrium geometries and corresponding minimum energies for $^{12}C^{16}O_2$, $^{13}C^{16}O_2$ molecules trapped in the two most probable sites, S1 and S2 of the fcc argon structure. The equilibrium orientations and displacement vectors of the molecule and the distortion vectors of the RG atoms of the first shell are schematized in Figure 4 for S1 and S2 substitutional sites, respectively.

In S1 site the equilibrium geometry is obtained when the molecular frame is identical to the crystal one *i.e.* the molecule axis is along one of the C_4 axis of the perfect lattice. The molecular c.m. lies in the site center. The maximum values of the distortion modulus of the matrix atoms are about 0.28 Å (about 7% of the site diameter). These values correspond to the displacement of eight atoms of the first shell. These atoms lie in two perpendicular planes containing the molecular axis. For the remaining four atoms of this shell which also lie in a plane (perpendicular to the above two planes), the distortion is smaller and is about 10% of the maximum values. Note that all these distortions correspond to matrix dilatation

around the molecule as shown in Figure 4a. Moreover as the distortion of the 2 groups of 4 atoms lying in two perpendicular planes containing the molecular axis are equivalent, then it is easy to understand why, in this site (S1), the ν_2 vibrating mode is still degenerate in the matrix.

In the double substitutional site (S2) the Oz molecular axis is collinear to the direction of the two substituted matrix atoms (twofold crystal axis). The molecular c.m. is free to move on both sides of the site center along the twofold crystal axis by about 0.92 Å. The maximum values of the distortion modulus of the matrix atoms are obtained for the four nearest neighbor atoms around the site center and are equal to 0.11 Å (about 1% of the site diameter). The remaining atoms of the matrices undergo distortions less than 0.03 Å. In this site, the distortions of atoms lying in two perpendicular planes containing the molecular axis are not equivalent and as anticipated (Sect. 2.2) in the discussion concerning experimental results, a lifting of the degeneracy of the ν_2 vibrating mode should occur in this site.

To fit experimental and calculated shift of ν_3 vibrational level (harmonic approximation) the first four shells around the trapped molecule have been progressively distorted. In S1, with respect to the site diameter, the matrix dilates with the first shell displaced by 17%, the second by 8%, the third by 4% and the fourth one by 2%. The overall distortion remain isotropic around the molecule. In S2, with respect to the mean site diameter (larger than for S1), the first shell is displaced by 6%, the second by 3%, the third by 1.5% and the fourth one by 0.7%. This time the distortion is not isotropic and is rather of cylindrical symmetry around the molecule. The matrix contracts along the molecular axis (C_2 axis) and dilates in the other two perpendicular directions.

Finally, in contrast with the ozone molecule trapped in rare gas matrices (8) for which the sites are equally probable, the energy minima connected to the single and double sites are different by about 20 cm^{-1} in Ar. This indicates that, at a temperature of 0 K, the trapping of the molecule in the double site is more probable than in the single one.

3.4.2 Harmonic vibrational frequencies

To determine the frequency shift, due to the matrix surroundings, of the fundamental vibrational modes of the molecule the first (β_i) and second derivative (β_{ij}) terms of equation (13) are first calculated for the equilibrium orientation of the trapped molecule and distortion of the matrix atoms and the resulting expression is introduced in equation (14). The new equilibrium configuration of the nuclei of the trapped molecule and the frequencies corresponding to the matrix distortion are then evaluated. The distortion around the molecule is thereafter adjusted to fit the observed and calculated (harmonic term) shift of ν_3. From the computed β_i and β_{ij} values, the harmonic and anharmonic vibrational potential constants are determined following the methods outlined above. The results are summarized in Tables 4, 5 and 6. Tables 4 give the

Table 4. First and second derivatives of the molecule-matrix interaction potential and dipole moment of isotopic CO_2 with respect to adapted normal coordinates.

$^{12}C^{16}O_2$/Ar fcc				
	S1		S2	
(cm^{-1})	0.0%	17.0%	0.0%	6.0%
β_1	-19.3887	4.5121	-0.8814	-2.3004
β_2	0.0000	0.0000	0.0000	0.0000
β_3	0.0000	0.0000	0.0000	0.0000
β_4	0.0000	0.0000	-7.6463	-2.9170
β_{11}	0.7140	-0.0296	0.1709	0.3080
β_{12}	0.0000	0.0000	0.0000	0.0000
β_{13}	0.0000	0.0000	0.0000	0.0000
β_{14}	0.0000	0.0000	0.2633	0.2810
β_{22}	0.2127	-0.6890	2.4935	-0.5641
β_{23}	0.0000	0.0000	0.0000	0.0000
β_{24}	0.0000	0.0000	0.0000	0.0000
β_{33}	0.2127	-0.6890	0.8584	-0.7186
β_{34}	0.0000	0.0000	0.0000	0.0000
β_{44}	-6.3702	-3.0951	-6.1783	-4.6492

$^{13}C^{16}O_2$/Ar fcc				
	S1		S2	
(cm^{-1})	0.0%	17.0%	0.0%	6.0%
β_1	-19.3849	4.5230	-0.8813	-2.3000
β_2	0.0000	0.0000	0.0000	0.0000
β_3	0.0000	0.0000	0.0000	0.0000
β_4	0.0000	0.0000	-7.4853	-2.9073
β_{11}	0.7137	-0.0311	0.1708	0.3078
β_{12}	0.0000	0.0000	0.0000	0.0000
β_{13}	0.0000	0.0000	0.0000	0.0000
β_{14}	0.0000	0.0000	0.2747	0.2932
β_{22}	0.2942	-0.6464	1.3400	-1.2394
β_{23}	0.0000	0.0000	0.0000	0.0000
β_{24}	0.0000	0.0000	0.0000	0.0000
β_{33}	0.2942	-0.6464	-0.1707	-1.3895
β_{34}	0.0000	0.0000	0.0000	0.0000
β_{44}	-6.0008	-2.8939	-5.8314	-4.3837

first and second derivatives calculated before (β_i and β_{ij}) and after (β_i' and β_{ij}') the fit of the ν_3 shift. In Table 5 are given the frequencies calculated for the three (four in site S2) vibrational modes of the molecule trapped in the two substitutional sites and in Table 6, the corresponding calculated shifts are compared to observed ones, the plus and minus signs characterizing the blue and red shifts, respectively.

We find by adjusting the shift of the strongest line, that those of the other lines are close to the observed shifts as shown in Table 6. For the ν_2 line, the same value is calculated for ω_2 and ω_3 for molecules in S1, but in S2 ω_2 and ω_3 differ by 0.34 cm^{-1}. Calculations in the harmonic

Table 5. Fundamental vibrational frequencies (in cm^{-1}) of isotopic species of CO_2 calculated at the harmonic approximation level in sites S1 and S2 before and after adjustment and harmonic frequencies in gas phase.

Molecule		$^{12}C^{16}O_2$		$^{13}C^{16}O_2$	
	Gas	1353.96		1353.96	
ω_1 (cm^{-1}) S1		1351.17	1354.39	1351.17	1354.39
S2		1353.73	1353.72	1353.73	1353.72
	Gas	672.88		653.73	
ω_2 (cm^{-1}) S1		675.45	671.00	656.40	651.94
S2		677.96	672.00	656.50	651.49
	Gas	672.88		653.73	
ω_3 (cm^{-1}) S1		675.45	671.00	656.40	651.94
S2		674.69	671.69	653.48	651.19
	Gas	2396.34		2328.14	
ω_4 (cm^{-1}) S1		2376.35	2391.84	2309.09	2323.99
S2		2383.65	2386.18	2316.15	2318.53

Table 6. Observed and calculated vibrational shifts frequencies (in cm^{-1}) of isotopic species of CO_2.

Molecule		$^{12}C^{16}O_2$		$^{13}C^{16}O_2$	
		Exp.	Cal.	Exp.	Cal.
$\Delta\omega_1$ (cm^{-1}) S1		–	$+0.83$	–	$+0.43$
	S2	–	$+0.16$	–	$+0.16$
$\Delta\omega_2$ (cm^{-1}) S1		-5.41	-1.88	-5.40	-1.79
	S2	-3.48	-0.88	-3.50	-2.24
$\Delta\omega_3$ (cm^{-1}) S1		-5.41	-1.88	-5.40	-1.79
	S2	-3.87	-1.19	-4.00	-2.54
$\Delta\omega_4$ (cm^{-1}) S1		-4.25	-4.50	-3.90	-4.15
	S2	-10.22	-10.16	-9.80	-9.61

approximation thus show, as expected that the splitting occurs in S2, the double substitutional site.

4 Conclusion

The splitting of the ν_2 vibrational mode has been observed from high resolution spectroscopic study of isotopic species of CO_2 trapped in argon. Line frequencies for the ν_2 and ν_3 vibrational mode for species containing ^{17}O atoms have been measured for the first time. A theoretical model is elaborated from a site inclusion model that allows an overall treatment of vibrational energies of the trapped molecule. Calculations show that CO_2 can be trapped in two different substitutional sites S1 and S2 as proposed by Irvine *et al.* [6]. In S2, calculations show that a splitting of the ν_2 vibrational mode occurs, a result which lead us to invert the attribution of reference [6]: the stable site is a single substitutional site whereas the unstable one is a double substitutional. Work is in progress concerning the

determination of the vibrational energies and the corresponding transition moments for $^{12}C^{16}O_2$, $^{13}C^{16}O_2$ and $^{14}N_2{}^{16}O$ trapped in argon, krypton and xenon matrices. In its present form, the theoretical model presented in this work can also be used to determine non-radiative relaxation rate constants of low-lying vibrational levels, by considering low frequency motions as a bath coupled to the vibrational degrees of freedom of the trapped molecule.

References

1. H. Chabbi, P.R. Dahoo, B. Gauthier-Roy, A.M. Vasserot, L. Abouaf-Marguin, M. Broquier, H. Dubost, R. Kolos, A. Tramer, J.M. Berset, J.M. Ortega, Chem. Phys. lett. **285**, 252 (1998).
2. L. Abouaf-Marguin, H. Chabbi, R. Dahoo, H. Dubost, B. Gauthier-Roy, D. Touahri, A.M. Vasserot, *International Conference on Chemistry and Physics in Matrices* (Austria, August 1997).
3. L. Fredin, B. Nelander, G. Ribbegard, J. Mol. Spectrosc. **53**, 410 (1974).
4. A. Loewenschuss, A. Givan, Spect. Lett. **10**, 551 (1977).
5. R. Guasti, V. Schettino, N. Brigot, Chem. Phys. **34**, 391 (1978).
6. M.J. Irvine, J.G. Mathieson, A.D.E. Pullin, Aust. J. Chem. **32**, 1971 (1982).
7. L.M. Nxumalo, T.A. Ford, J. Mol. Struct. **327**, 145 (1994).
8. P. Brosset, R. Dahoo, B. Gauthier-Roy, L. Abouaf-Marguin, A. Lakhlifi, Chem. Phys. **172**, 315 (1993).
9. P.R. Dahoo, Research Habilitation, University of Versailles (1997) and references therein.
10. J.H. van Vleck, Phys. Rev. **33**, 467 (1929).
11. H.H. Nielsen, Rev. Mod. Phys. **23**, 90 (1951).
12. A. Lakhlifi, C. Girardet, R. Dahoo, P. Brosset, B. Gauthier-Roy, L. Abouaf-Marguin, Chem. Phys. **177**, 31 (1993).
13. A. Lakhlifi, R. Dahoo, M. Vala, J. Szczepanski, S. Ekern, Chem. Phys. **222**, 241 (1997).
14. A. Lakhlifi, C. Girardet, J. Mol. Struct. **110**, 73 (1990); M.L. Klein, J.A. Venables, in *Rare Gas Solids* (Academic Press, London, 1976), Vol. I.
15. M.E. Rose, in *Elementary Theory of Angular Momentum* (Wiley, New York, 1967).
16. J.L. De Coen, G. Elefante, A.M. Liquori, A. Damiani, Nature **216**, 910 (1967).
17. C.S. Murthy, K. Singer, M.L. Klein, I.R. McDonald, Mol. Phys. **41**, 1387 (1980), *ibid.* **44**, 135 (1981).
18. D.E. Stogryn, A.P. Stogryn, Mol. Phys. **11**, 371 (1966).
19. J.L. Teffo, Ph.D. thesis, University of Paris VI, (1990) and references therein.
20. P.A. Flinn, A.A. Maradudin, Annals Phys. **18**, 81 (1962).
21. E.B. Wilson Jr., J.C. Decius, P. Cross, in *Molecular Vibrations* (Dover Pub., 1980).
22. R.C. Herman, W.H. Shaffer, J. Chem. Phys. **16**, 453 (1948).
23. G. Amat, H.H. Nielsen, Chem. Phys. **27**, 845 (1957).
24. S.C. Wang, Phys. Rev. **34**, 243 (1929).